as $\mathbf{A}_i =$

$$\begin{bmatrix} A_{00} & A_{01} & 0 & \cdot & \cdot & \cdot & & & \\ A_{10} & A_{11} & A_{12} & 0 & \cdot & \cdot & \cdot & & \\ A_{20} & 0 & A_{22} & A_{23} & 0 & \cdot & \cdot & \cdot & \\ A_{30} & 0 & 0 & A_{33} & A_{34} & 0 & \cdot & \cdot & \cdot \\ \cdot & \cdot & \cdot & \cdot & \cdot & & & & \\ A_{N,0} & 0 & \cdot & \cdot & \cdot & 0 & A_{N,N} & & \\ A_{N+1,0} & 0 & \cdot & \cdot & \cdot & 0 & A_{N+,1N} & A_{N+1,N+1} & \end{bmatrix} \tag{45}$$

This problem is solved by matrix inversion using the same numerical values used in Example 5-1 of Holland (3). The temperature is again obtained by solving Equation (30) using Newton's method. The initial approximations or starting values listed in Equation (40) are again used. The convergence rates of the distillate flow rate and distillate composition are listed in Table 5.* In spite of the very approximate starting values used, only seven iterations are needed to obtain a D value of 48.93. Eleven iterations are needed to obtain a D value of 48.90.

DISCUSSION

The quasilinearization technique is a useful tool for solving the equations representing multicomponent distillation. The basic idea is to consider the equations formulated in multicomponent distillation as nonlinear boundary-value problems in difference equations. Thus the various techniques used in solving nonlinear boundary-value problems in differential equations can be used to solve problems in multicomponent distillation.

The decoupling scheme used in obtaining Equations (42) and (43) from Equations (23) and (25) appear to have slowed down the convergence rate. However, the convergence rate in Table 5 is still about the same as the convergence rate given by Holland by the use of the θ method, in spite of the fact that a better initial approximation was used by Holland.

Since the idea of considering the distillation problem as nonlinear boundary-value problem is very general, various approaches or formulations can be used to solve this problem. For example, the formulation represented by Equations (1) through (4), which are obtained by considering material balance around each individual plate, can also be used for solving problems with variable flow rates. The equations used in the Thiele and Geddes method form another starting point for the application of the quasilinearization concept. Perhaps the most important advantage in the nonlinear boundary-value and quasilinearization approach is that it can be used to solve complex columns with several feed plates and withdrawn streams in the same way as that used to solve simple or conventional distillation columns.

ACKNOWLEDGMENT

The work was partially supported by the National Air Pollution Control Administration, Consumer Protection and Environmental Health Service, U. S. Public Health Service, Department of Health, Education, and Welfare Grant No. AP 00895-01.

LITERATURE CITED

1. Lee, E. S., "Quasilinearization and Invariant Imbedding," Academic Press, New York (1968).
2. ———, AIChE J., **16**, 679 (1970).
3. Holland, C. D., "Multicomponent Distillation," Prentice-Hall, Englewood Cliffs, N. J. (1963).
4. Fort, T., "Finite Differences and Difference Equations in the Real Domain," Oxford Univ. Press, London (1948).
5. Milne-Thomson, L. M., "The Calculus of Finite Differences," Macmillan, London (1933).

Manuscript received January 29, 1970; revision received April 27, 1970; paper accepted May 18, 1970.

---

* See footnote on page 887.

Kinetics and Deactivation on Large Catalytic Particles

STEVEN KOESTENBLATT and EDWARD N. ZIEGLER

Department of Chemical Engineering
Polytechnic Institute of Brooklyn, Brooklyn, New York 11201

Solids of ⅛ in. or larger nominal size are often used in chemical reaction processes as either reactant or catalyst particles. If the particle dimensions or geometry of such particles are altered, the overall reaction rate may change owing to the influence of pore diffusion and/or thermal gradients. The latter effect will be most pronounced for highly exothermic reaction rate-controlling situations because of the sensitivity of rate constants to temperature. It has significance regardless of the rate-controlling mechanism, however, and may alter the catalyst behavior as a result of localized degradation at reactor hot spots. For analyzing the kinetics of an exothermic reaction, one would ideally prefer isothermality in the reactor, a condition difficult to achieve because of the poor effective thermal conductivity of packed gas-solid systems. To overcome the temperature problem, many processes have been switched to fluidized-bed operation in which the particles are ground or crushed to a smaller size and suspended by the reactant gases. Although heat transport throughout the bed is improved by this technique, bubble formation and backmixing reduce the overall conversion. The packed-bed reactor has thus remained the mainstay of gas-solid reactive contact. For fairly exothermic reactions an exchanger or a jacketed reactor can maintain the temperature rise within prescribed limits, but are not adequate for obtaining the degree of isothermality required of kinetic analysis for large size particle systems. Fluidizing inerts in a packed-bed reactor

---

Correspondence concerning this article should be addressed to Prof. E. N. Ziegler. S. Koestenblatt is with Esso Systems and Mathematics, Florham Park, New Jersey 07932.

seems more promising for kinetic studies.

Integral bed situations with fluidized particles in the interstices have been studied, but not for the purpose of kinetic analysis. Argonne National Laboratory (*1*) has developed a volatility process in which large (½-in.) uranium dioxide pellets are fluorinated using interstitially fluidized inert particles to enhance heat removal. Ishii and Osberg (*2*) have investigated the effect of inert packing on the isomerization of cyclopropane on catalytic fluidized particles, where the packing is used primarily to improve gas-catalyst contacting.

In this work the exothermic hydrogenation of ethylene is studied on two types of large size packed catalysts with smaller inert solid particles suspended by the reactants, to determine the uniformity of temperature around the outer catalyst surface and to determine the feasibility of kinetic studies by this means of catalyst testing. It is intended to achieve inter- rather than intraparticle isothermality, although in all but pore diffusion controlled reactions it is expected that uniform temperatures might be attained within the particles as well. The consequences of deactivation and catalyst conditioning are also investigated.

The hydrogenation of ethylene in the presence of metallic catalysts, especially nickel, has been the subject of intensive investigations, as a prototype of catalyzed hydrogenations of the sort, since its discovery by Sabatier and Sanderens in 1897 (*3*). The simple overall reaction

$$\begin{gathered} H_2 + C_2H_4 \xrightarrow{\text{cat.}} C_2H_6 \\ A + B \xrightarrow{\text{cat.}} C \end{gathered} \tag{1}$$

belies the difficulties in obtaining a satisfactory mechanism for the conversion. Rates of the catalyzed reaction often decline markedly and apparently uncontrollably on repetition of the runs over the same catalyst, because of such factors as impurities in the reactants and the polymerization or chemisorption of various species on the catalyst. The character of catalyzed hydrogenation depends further on the form and condition of the catalyst.

An equilibrium constant-temperature (K atm.$^{-1}$ versus T°K.) has been developed by Pease (*5*).

TABLE 1. SUMMARY OF THE REACTION KINETICS OF THE HYDROGENATION OF ETHYLENE

Catalyst (Reference)	Initial conditions	Type of test	Reaction mechanism and/or rate equation with activation energy
Nickel foil (*6*)	73° to 200°C. $P = 12$ cm. Hg	C_2H_4, H_2	$r \alpha p_B$, hydrogen in excess $r \alpha p_A$, ethylene in excess
Nickel-on-charcoal (*7*)	−84° to 50°C.	C_2H_4, H_2	$r \alpha p_A$
Nickel wire (*8*)	20° to 250°C. $p_A = 7$ to 20 mm. Hg $p_B = 10$ to 30 mm. Hg	C_2H_4, H_2, HD	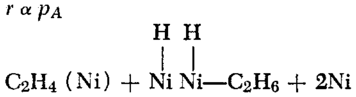 $C_2H_4\,(Ni) + \overset{H\;\;H}{\overset{\vert\;\;\;\vert}{Ni\;Ni}}\!-\!C_2H_6 + 2Ni$
Nickel wire (*9*)	−10° to 120°C. $P = 0.03$ mm. Hg	C_2H_4, H_2	$r \alpha p_A$, at constant p_B $r/p_A \alpha p_B/(1 + Kp_B)$ at constant p_A
Nickel powder (*10*)	−78° to 0°C. $p_A, p_B = 10$ to 130 mm. Hg	C_2H_4, H_2	$r \alpha p_A, p_B$ constant
Nickel wire (*11*)	99° − 165°C. $p_A, p_B = 100$ to 400 mm. Hg	C_2H_4, H_2	$r \alpha p_B/(1\ Kp_B)$, p_A constant
Nickel wire (*12*)	156°C.	C_2H_4, D_2	$r \alpha p_A$ 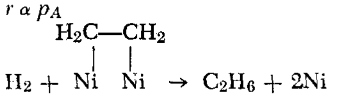 $H_2 + \overset{H_2C\text{—}CH_2}{\overset{\vert\;\;\;\;\;\vert}{Ni\;\;\;Ni}} \rightarrow C_2H_6 + 2Ni$
Evaporated nickel film —carbided (*13*)	20° to 170°C. $p_A = 2$ to 10 mm. Hg $p_B = 2$ to 10 mm. Hg	C_2H_4, H_2	$H_2 + Ni_2 \rightarrow H_2\,(Ni_2)$ $C_2H_4 + H_2(Ni_2) \rightarrow C_2H_6 + Ni_2$ $r \alpha p_A$, 114°C. $r \alpha p_Ap_B/(1 + Kp_B)$, 170°C.
Evaporated nickel film (*14*)	−80° to 150°C. equimolar mixture	C_2H_4, H_2	$C_2H_4 + 2HNi \rightarrow C_2H_6 + 2Ni$ $r \alpha p_A$
Evaporated nickel film (*15*)	−100°C. $p_A = 8.1$ mm. Hg $p_B = 2.7$ mm. Hg	C_2H_4, D_2	$r \alpha p_A{}^{1/2}$
Nickel-on-alumina —carbided (*16*)	70°C. $P = 1$ to 5 atm. $y_{Ai} = 0.40$ to 0.90	C_2H_4, H_2	$r \alpha p_Ap_B/(1 + Kp_B)$
Evaporated nickel film —carbided (*17, 18*)	−23° to 160°C. $P = 20$ mm. Hg equimolar mixture	C_2H_4, D_2	$r \alpha p_A$
Nickel plate (*19*)	36° to 85°C. $p_A > p_B$ $= 0.02$ to 21.7 mm. Hg	C_2H_4, H_2	$r \alpha p_A$
Evaporated nickel film (*20*)	−40° to 40°C. $p_A = 98$ mm. Hg $p_B = 49$ mm. Hg	C_2H_4, H_2	$r \alpha p_A$
Nickel Kieselguhr (*21*)	156°C. $p_A = 60$ mm. Hg $p_{D_2} = 60$ mm. Hg equimolar with ethylene	C_2H_4, H_2, D_2	$Ni + C_2H_4 \rightleftarrows C_2H_4\,(Ni)$ $C_2H_4\,(Ni) + H_2\,(Ni) \rightleftarrows C_2H_5\,(Ni) + H\,(Ni) \rightarrow C_2H_6$ $r \alpha p_A$
Nickel wire (22)	62° to 200°C. $p_A = 38$ to 304 cm. Hg $p_B = 38$ to 684 cm. Hg	C_2H_4, H_2	$H_2\,(Ni) + C_2H_4\,(Ni) \rightarrow C_2H_6 + 2Ni$ $r \alpha p_A$

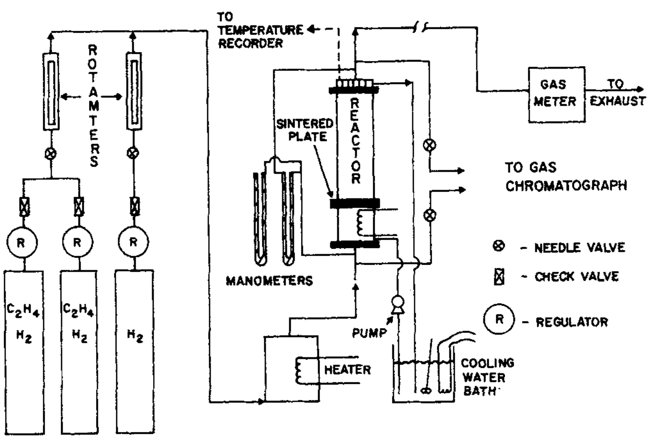

Fig. 1. Flow diagram of system.

$$\log K = 6774/T - 3.408 \log T + 0.000809T + 3.120 \tag{2}$$

It may be concluded that the equilibrium at and below 400°C. greatly favors the hydrogenation reaction.

The research activity involving the rate and mechanism of ethylene hydrogenation has been formidable as may be inferred from the summary of many investigations presented in Table 1. Using mixtures of light and heavy hydrogen, Farkas et al. (*8*) discovered by a thermal conductivity analysis that an exchange reaction

$$C_2H_4 + HD \rightarrow C_2H_3D + H_2 \tag{3}$$

occurred along with the addition reaction

$$C_2H_4 + HD \rightarrow C_2H_5D \tag{4}$$

with similar behavior expected of pure D_2 or H_2 in the feed.

Beeck (*14*) also found that ethylene adsorbs readily and self hydrogenates to ethane at 23°C., suggesting a dissociative adsorption giving adsorbed hydrogen, possibly in atomic form, and an acetylene residue with properties unlike those of adsorbed acetylene.

$$C_2H_4 + 4Ni \rightarrow Ni_2(C_2H_2) + 2\,H\,Ni \tag{5}$$

The formation of ethane would then occur by the rapid reaction between adsorbed hydrogen and gaseous ethylene.

$$C_2H_4 + 2\,H\,Ni \rightarrow C_2H_6 + 2\,Ni \tag{6}$$

Using alumina-supported nickel catalyst, Pauls et al. (*16*) obtained flow reactor data at 1 to 5 atm. pressure and temperatures between 30° and 80°C., which could be represented by a rate expression of the form

$$-r_B = Ap_Ap_B/(1 + Bp_B) \tag{7}$$

with an activation energy of 11.6 kcal./mole, which is typical of a reaction-controlled rate process.

The overall reaction rate is inhibited by residue formation (carbided surface), but can be improved reproducibly by pretreatment with pure hydrogen at 5 cm. Hg and 250°C. (*27*). Perhaps the retardation may be caused by the decrease in hydrogen adsorption on carbided surfaces observed by Miyahara (*17, 18*). The apparent activation energy increases with increased residue formation (*19*).

Crawford etal. (*20*) and Cormack et al. (*28*), by independent techniques, arrived at the conclusion that surface heterogeneities toward ethylene and hydrogen exist, supporting Beeck's (*14*) contention that the hydrogenation reaction takes place on portions of the surface not covered by strongly adsorbed species. The model of an adsorbed hydrogen atom adding to an associatively adsorbed ethylene molecule through an ethyl radical intermediate was first postulated by Horiuti and Polanyi (*29*). Farkas (*30, 31*) hypothesized a dissociative hydrogen adsorption rate-controlling step with a separate dissociative ethylene exchange reaction.

Jenkins and Rideal (*13*) postulated both an ethylene dissociation to acetylenic complexes and hydrogenation by the combination of gaseous ethylene with chemisorbed hydrogen. No associative adsorption (simple chemisorption) of ethylene was observed and the steady state rate equation developed was

$$r = k_1\,k_3\,p_A\,p_B/(k_2 + k_3\,p_B + k_1\,p_A) \tag{8}$$

By assuming that $k_3p_B >> (k_2 + k_1\,p_A)$, a rate equation which is first order in hydrogen and zero order in ethylene was rationalized, which is in agreement with the data at temperatures below 160°C. However, an equation of similar form cited by Eley (*32*) may also be developed from the Horiuti and Polanyi mechanism. The proper mechanism cannot be distinguished by rate data alone. Further discussion of the hydrogenation mechanisms may be found elsewhere (*33*). Some verification of the above postulate for large particle systems is attempted.

EXPERIMENTAL APPARATUS

Reactant gas mixtures were metered and preheated while being fed to the fluidized packed-bed reactor, as in the flow diagram of Figure 1. Flow rates of hydrogen and hydrogen-

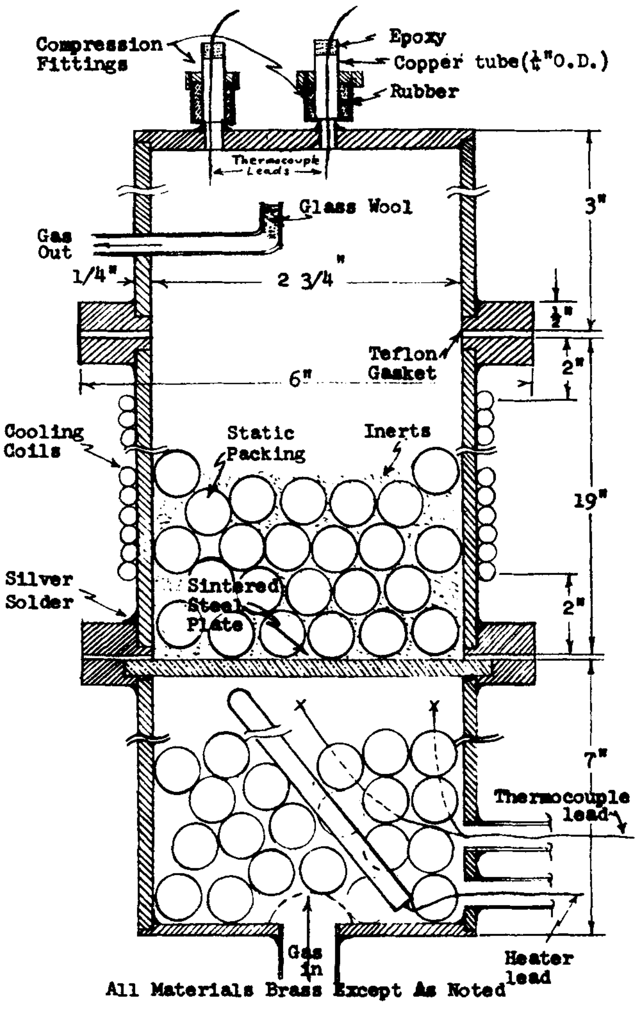

Fig. 2. Reactor schematic.

ethylene mixtures were measured to within ± 1.5% by rotameters which were calibrated using a wet-test meter and timer. The rotameter flow capacities were 0 to 60 cu. ft./hr. ethylene, 0 to 40 cu. ft./hr. hydrogen, and 0 to 40 cu. ft./hr. of a 27% ethylene in hydrogen mixture, all flows corrected to STP. The heating section was constructed by winding a 500-w. insulated michrome heating tape about a ¼-in. diam. helically coiled copper tube.

The heart of the system was a 2.75-in. diam. (I.D.) brass tubular reactor cut to a length of 30 in. with flanges to support a sintered steel distributor and to connect with the preheat and exit sections. The flanges were constructed of brass plate and silver-soldered to the reactor tube and Teflon-covered asbestos gaskets were used (good to 250°C.). The vessel was filled with catalyst and inerts and was wound with 0.25-in. diam. tubing for water cooling and with asbestos-covered michrome wire for heating. The external gaps were filled with a high temperature heat transfer cement to provide a uniform heat flux and the hardened mixture was insulated with a 1.5-in. thick asbestos covering. An insulated 8-in. gas distribution section preceded the reactor. It contained a 250-w. cartridge heater which was used if additional preheat was required. A reactor cross section is presented in Figure 2. Copper-constantan thermocouples were introduced through compression fittings at the exit flange to five bed positions, arranged as a cross to give some indication of both lateral and radial thermal gradients, and in the gas phase of the distributor for inlet temperature measurements. Small holes were drilled a short depth into the catalyst packing and served as a container for thermocouple beads which were fixed in position by epoxy.

The reaction rates were determined using composition analyses at the reactor inlet and outlet streams obtained with a Perkin-Elmer 154 L thermal conductivity gas chromatograph and a 3-ft. silica gel column operated at 32°C. with an 8.5% hydrogen-helium carrier gas at 4 lb./sq. in. gauge. The chromatograph was calibrated using the responses to premixed gas samples obtained on a 1-mv. recorder attenuated to full scale. The mole fractions of ethylene and ethane could be consistently related to their peak areas, but not to their heights. The areas were subsequently determined with a planimeter, and run-to-run calibrations using the area of a single sample were sufficient. Reproducibility was precise to within 1%, but calibrations were made before and after each data set to correct for drifts due to chromatograph temperature and sample flow rate. The hydrogen adsorbed and desorbed rapidly and appeared 20 sec. after sample entrance. The ethylene and ethane peaks were more difficult to separate and the 32°C., 4 lb./sq. in. gauge conditions were found after some experimentation. Ethane appeared at about 3 min. and ethylene at about 6 min. after entrance. The sample volume fed to the chromatograph was maintained constant at room temperature and ¼-in. H_2O gauge pressure by using a vessel with ¼-in. H_2O above the outlet tube and then pinching shut a rubber connective tube to the chromatograph. The silica gel was regenerated periodically with nitrogen at 185°C. and 25 lb./sq. in. gauge.

Temperature control for the hydrogenation is essential for accurate kinetic results, preliminary calculation indicating that a 1°F. rise would cause a 3% change in reaction rate. Manual control of the reactor temperature was tried, but it was difficult to attain a steady temperature, probably because of room temperature changes and drafts. Water from a controlled temperature (±0.25°F) bath was preheated to just below the desired reactor temperature and centrifugally pumped through a 10r to 30r heater combination maintaining the average steady reactor temperature during a run to < 1.0°F.

MATERIALS AND THEIR PREPARATION

The catalyst was prepared by depositing nickel from an aqueous solution of the nitrate on graded 0.375- and 0.5-in. 99.5% aluminum oxide balls (Alcoa T 162) having a surface area of 0.04 sq. m./g. and pore volume of 0.015 ml./g. Another carrier of activated bauxite (Phillips Corp. Porocell) 88% aluminum oxide, 200 sq. m./g., was machined to ½ × ½ in. cylinders. The catalyst was prepared by a method similar to the one used by Pauls, Coming, and Smith (*16*). For the alumina catalyst an aqueous solution of nickel nitrate was prepared by dissolving 1 lb. of reagent grade $Ni(NO_3)_2 \cdot 6H_2O$ in 500 ml. of distilled water forming a solution which contained approximately 15 g. of nickel/100 ml. water. The solution was added to a flask containing the carrier balls, where they remained for 24 hr. with intermittent agitation. After this period the balls were removed from the solution and allowed to drain for 30 min. before being placed in a porcelain pan and dried for 4 hr. at 110°C. The nitrate was decomposed by placing the balls in a furnace at 400°C. for 12 hr. The oxide was finally reduced by allowing hydrogen to flow over the catalyst in the reactor at a rate of 3 cu. ft./hr. for 24 hr. at 250°C. The production of water was observed to cease after 6 hr. using a Drierite column at the effluent.

The Porocell catalyst was prepared in the same manner as the alumina except that a nickel solution with 10 g. of nickel/100 ml. of water was used to impregnate the carrier. Also, a batch of this catalyst was prepared by placing the cylinders in a flask under vacuum during the impregnation period. Originally a few batches of the alumina catalyst were prepared using the same procedure and nickel solution as the Porocell catalyst, but the alumina catalyst prepared with the 10 g./100 ml. concentration produced an undesirably small conversion of ethylene to ethane.

The hydrogen gas used in the reduction of the catalyst and the kinetic experiments was a prepurified grade; the ethylene was C.P. grade. The hydrogen had a minimum purity of 99.95% and contained less than 20 p.p.m. of oxygen and the ethylene purity was >99.5% with a remainder of inerts. The prepared mixtures of 27% ethylene in hydrogen were made from these two grades and were used in the majority of runs, since expansion across the valve leading from the pure ethylene tank caused the regulators to freeze, continually changing the ethylene flow rate.

The inert fluidized particles used throughout this study were borosilicate glass beads obtained from the La Pine Scientific Company. These microspheres had a size range of 62 to 82 μ (−170 +230 mesh) and were used as received. The beads had a bulk specific gravity of 1.5 and a density of 2.5 g./cu. cm. The particles were of a size compatible with the packing size as was recommended for high heat transport rates (*34*).

During each run the rotameter readings, pressure at the reactor inlet and in the room, pressure drop through the vessel, temperatures in the reactor, circulating water, and room, and back up wet-test meter readings were all recorded. The most reproducible data were obtained by treating with reactant mixture at 90°C. for 8 hr. before a series of runs. The feed gas composition was varied between 5 and 28% ethylene and the total flow rate from 0.051 to 0.22 cu. ft./min. at 1 atm. and 0°C.

The reaction rate expressed as the formation rate of ethylene r_B can be written in terms of ethane mole fraction assuming no ethane is present initially and accounting for the mole change during reaction. Thus, for a differential mass of catalyst dW, assuming plug flow, it is reasonably simple to show that

$$-r_B = \frac{1}{(1+y_C)^2}\,\frac{dy_C}{d(W/F_o)} \tag{9}$$

The mole fractions for ethane and hydrogen may be expressed in terms of y_C as follows

$$y_A = y_{Ai} - y_C\,(1 - y_{Ai}) \tag{10}$$

$$y_B = y_{Bi} - y_C\,(1 - y_{Bi}) \tag{11}$$

and the total molar flow rate as

$$F = F_o/(1 + y_C) \tag{12}$$

By assuming perfect mixing the rate of reaction may be readily derived as

$$-r_B = \frac{1}{(1+y_C)_{\text{out}}}\,\frac{(y_C)_{\text{out}}}{(W/F_o)} \tag{13}$$

if no ethane is present initially. The reactor operation at 50.5°C. could be considered differential since ethylene conversion was < 7%, and the temperature variations were minimized by the fluidized particles. The difference between the

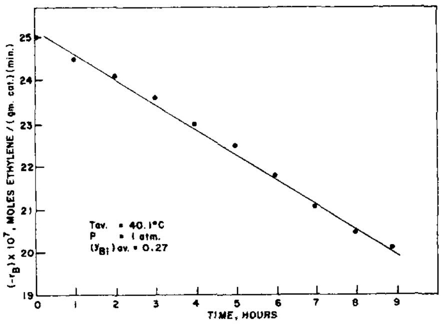

Fig. 3. Effect of conditioning on reaction rate (no preconditioning).

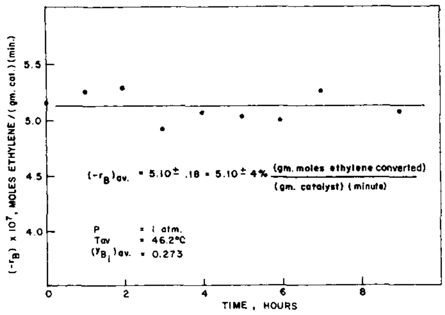

Fig. 4. Effect of conditioning on reaction rate (6 hr., 170°C., reactant mixture).

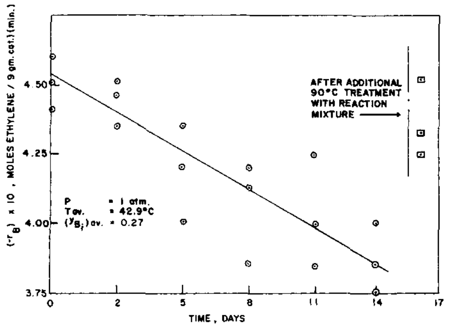

Fig. 5. Deactivation of conditioned alumina catalyst (6 hr., reactant mixture, 170°C.).

rates calculated from Equations (9) and (13) is less than ½%, and hence independent of the mixing conditions within the reactor. It was assumed in Equation (9) that the average value of $(1 + y_C)$ could be used and that $dy_C/d(W/F_o) = y_C/(W/F_o)$. The average reaction rate was considered for convenience to correspond to the mean concentrations in the reactor producing an error of 3% in the worst instance for ethylene deviations.

DEACTIVATION RESULTS AND DISCUSSION

Both unimpregnated alumina and the glass beads were tested and found to be noncatalytic. The pure gas-phase reaction rate was calculated to be many orders of magnitude lower than the observed catalytic rate.

A series of tests was run to determine the stability of the 15 g. nickel/100 ml. of aqueous nitrate solution on alumina catalyst surface with relation to the various reactants. The inlet gas flow was approximately 0.05 cu. ft./min. (at 0°C. and 1 atm.) in a column of inert beads filled to a stationary height of 6 in.

Figure 3 is a plot of reaction rate versus time for the alumina catalyst which has been cooled to the desired reaction temperature of 40.1°C. while hydrogen continued to flow through the reactor. After passing the reaction mixture, at the reaction temperature, over the catalyst for 24 hr. the results in the figure were obtained. Over a period of 10 hr. the reaction rate declined from 25.1 to 20.7 × 10^{-7} g.-moles ethylene converted/g. catalyst/min. and a similar decline in the extent of conversion was also noted. This decline is approximately 20% of the initial reaction rate recorded and the catalyst surface is apparently unstable and therefore unsuitable for kinetic studies.

In order to stabilize the surface, a conditioning process was sought. The literature (*13, 16*) mentions two methods of conditioning catalyst to produce a stable surface. Both processes involve treating the catalyst at 170°C., but one suggests using pure ethylene, while the second suggest using the reaction mixture itself. As a second method was applied to a nickel-on-alumina catalyst this method was adopted. The rationale for using 170°C. is that a reaction such as carbidization may be rapidly completed and is only moderately reversible at about 40°C. Figure 4 is a plot of the results obtained after conditioning the catalyst with reaction mixture at 170°C. for 6 hr. upon completion of the reduction period, for which the mixture was then allowed to pass over the catalyst at 40°C. for 24 hr. From Figure 4 it can be inferred that there was no rapid deactivation of the catalyst after the conditioning process. The catalyst surface was apparently stable, and therefore satisfactory for future work in studying the kinetics of ethylene hydrogenation. The reproducibility of data within a batch was good; relative standard deviation at a nominal condition was about 4%. The catalyst was not repacked at any time, partially because exposure deactivates the catalyst. The reproducibility of data in different batches was not expected to be good because the activity is very sensitive to the concentration of nickel.

The reaction rates for the runs conditioned at 170°C. with the reaction mixture were about one fifth as large as the nonconditioned runs. Apparently, whatever poisoning took place on the catalyst surface occurred more rapidly at 170°C. than at 40°C. and appears to have been curtailed by the conditioning process. A major difference between the two processes is the inclusion of ethylene in the gas mixture passing over the catalyst at 170°C. Ethylene appears to deactivate the catalyst with the process being accelerated at 170°C. to a steady state condition.

This result can be explained by a model proposed by Jenkins and Rideal (*13*) for the poisoning of pure nickel films by ethylene. They suggest that ethylene is dissociated upon chemisorption to an acetylenic complex and chemisorbed hydrogen. The chemisorbed hydrogen then reacts with gas-phase ethylene (self-hydrogenation) leaving two vacant sites (*14, 35, 36*). Another molecule of ethylene may be chemisorbed and converted into a complex, this process continuing until all the groups of four sites that are capable of adsorbing ethylene are utilized. According to the proposed model the remaining sites, those unable to chemisorb ethylene, are available for the hydrogenation reaction. Later investigators (*20, 27, 28*) have verified the model and suggested that the nickel catalyst surface consists of two parts: one which catalyzes the dehydrogenated adsorption and the other the hydrogenation reaction.

With the procedure used in this work, the carbided surface postulated is probably the stable surface attained. The surface of particles removed from the reactor contained a dark powdery substance not present on the catalyst originally. When a typical sphere was halved, a thin dark shell of penetrated material was discovered, with the remainder of the sphere having the white color of fresh catalyst. Although the catalyst is nominally stable, long-term deactivation is found as in Figure 5 for which the expanded scale accentuates some of the scatter in the data. The compound interest formula used for reaction rate decay

$$r = r_o/(1 + a)^t \tag{14}$$

may be used to correct for runs taken over long periods of time without reactivation. By reconditioning at 90°C. some of the delayed deactivation appears to be counteracted.

Direct ethylene poisoning was studied using the ⅜-in. alumina spheres. The catalyst was again conditioned at 170°C. for 6 hr. with 27% ethylene in hydrogen reaction mixture followed by a 24-hr. pure ethylene treatment at 0.04 cu. ft./min. STP flow rate. Reaction temperatures were maintained at 51°C. with average STP flow rates

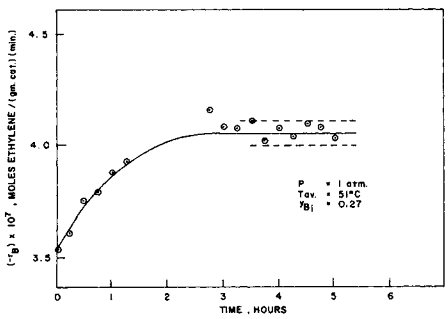

Fig. 6. Effect of ethylene treatment on reaction rate.

of 0.051 cu. ft./min. The reaction rate increased with increasing time to a constant level in the manner depicted in Figure 6. A similar study was carried out for a pure hydrogen pretreatment at an STP flow of 0.11 cu. ft./min., followed by reaction at 60°C. and 0.63 cu. ft./min. Figure 7 is a plot of the results of hydrogen pretreatment from which it is clear that reaction rate decreases sharply with increasing time approaching a constant level.

By placing the catalyst in the ethylene atmosphere, the surface probably became saturated with acetylenic complexes which occupied sites otherwise available for reaction. Apparently these new complexes are not tightly held on the surface as they are removed by reaction mixture. The pure hydrogen treatment, where the rate is initially higher than expected, supports the concept. The hydrogen removes the complexes from the catalyst surface and the introduction of reaction mixture enables the complexes to reform their bonds with active sites.

A series of rates for runs at two different feed compositions is presented in Figure 8. The reaction was approached first by using an inlet ethylene concentration, $y_{Bi} = 0.26$ for 5 hr., then switching to $y_{Bi} = 0.21$ (section X_1), and finally to $y_{Bi} = 0.174$ (section Y_1). The situation is then reversed by starting with $y_{Bi} = 0.174$ (section Y_2) and returning to $y_{Bi} = 0.21$ (section X_2). The gas flow rates for sections Y were 0.151 std. cu. ft./min. and for sections X, 0.112 std. cu. ft./min. In going to section X_1 the rate increases, and to section X_2 it decreases. In section X_1 the mole fraction of ethylene was reduced from the previous value and for section X_2 it was increased from the previous value. There may exist a near-equilibrium state between the adsorbed poison and the ethylene in the gas phase. Thus, when the ethylene level in the gas phase is reduced, that on the solid also decreases, making more active sites available and increasing the reaction rate. Unlike the conclusions drawn from the data of Jenkins and Rideal (*13*) then, it appears that only a portion of the surface remains carbided while another portion is able to absorb or desorb its carbides or complexes which changes the overall rate. This may be explained on the basis of a site activity distribution with only the most active sites retaining the complex under reducing conditions.

In an attempt to insure steady state operation for the kinetic studies, the catalyst was conditioned for 6 hr. at 170°C. with reaction mixture, followed by a 90°C. pretreat. The inlet mole fraction over the series was lowered unidirectionally from one run to the next, each taking from 3 to 5 hr. to attain a steady state. After each day of operation, the original condition was rerun to check for unexpected activity changes.

The rate of ethylene hydrogenation was found to increase with increasing temperature according to an Arrhenius relationship, as in Figure 9, for temperatures which were varied from 40° to 90°C. and velocities from 0.047 to 0.19 std. cu. ft./min. The average inlet mole fractions of ethylene were 0.258 and 0.272, the reaction rates were velocity averaged, and the reaction temperature calculated by taking the average of inlet and outlet reactor temperatures. The largest deviation from the mean temperature was 0.5°C. The reaction rate was calculated by averaging the results of three runs at three different gas velocities. A complete set of data and calculations may be found elsewhere (*37*). A reproducibility check was made after a few weeks and the activation energy remained constant at 10.3 kcal./mole in agreement with previous investigators (*13, 16, 17, 19*). The average deviation within a run is about 6% but the absolute value decreased after two weeks, presumably as a result of deactivation, perhaps caused by the small increase in average inlet ethylene concentration.

Although deposits of high carbon/hydrogen compounds seem to form almost entirely within a thin outer shell, deactivation by pore blockage seems improbable. If the pores were partially blocked, diffusion to active sites would become rate controlling, and the apparent activation energy would be expected to decrease. Since the catalyst activation energy maintained itself after two weeks while its activity was reduced, it might be speculated that poisoning of a fraction of the sites occurred.

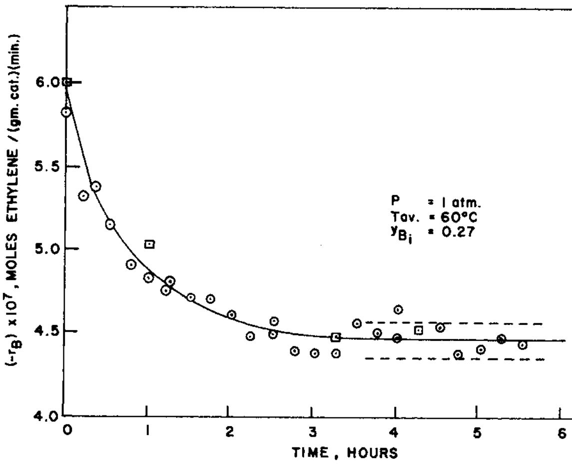

Fig. 7. Effect of hydrogen treatment on reaction rate.

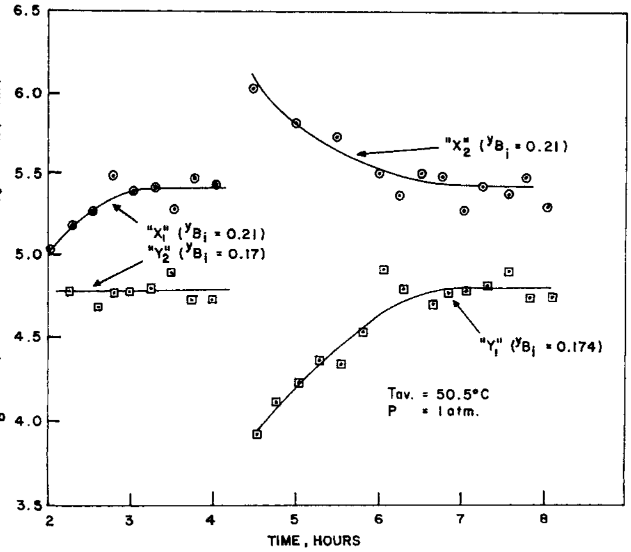

Fig. 8. Effect of catalyst treatment on reaction rate.

As the Arrhenius relationship was unaffected by temperature the rate may be described as a product of two functions

$$-r_B = f(C)\,g(T) \tag{15}$$

one dependent solely on concentration and the other on temperature alone. The value of 10.3 kcal./mole was used to correct the runs through Arrhenius function $g(t)$ for small differences from the nominal temperature. Comparable runs with a packed bed having no interstitially fluidized particles produced large temperature gradients (about 20°C.) and could not be used for establishing a rate versus temperature relationship.

The concentration function was developed from initial rate data using a nominal temperature of 50.5°C. with gas flow 0.0511 to 0.217 std. cu. ft./min., inlet compositions from 5 to 28% ethylene, and 1.0 to 1.25 atm. pressures. The reactor was packed with 486 g. of ⅜-in. catalyst (about 6 in. of reactor height) which was then covered with 700 g. of fine glass beads. The catalyst was first conditioned at 170°C. with 28% ethylene in hydrogen mixture, followed by 24 hr., 90°C. treatment between each set of runs. The largest temperature difference observed in all the runs, including both axial and radial directions, was only 0.8°C. An average temperature was therefore defined as the arithmetic mean of inlet and outlet temperatures. The mechanism of the Longmuir-Hinshelwood or Longmuir-Rideal type which best fits the data is the reaction between gaseous hydrogen and adsorbed ethylene, with negligible ethylene adsorption,

$$-r_B = kp_A p_B/(1 + K_B p_B) \tag{16}$$

where $k = 1.34 \times 10^{-5}$, $K_B = 23.3$, both at 50.5°C., with partial pressure expressed in atmospheres and rate in gram-moles of the ethylene formed per gram of catalyst per minute. The largest deviations of the correlation, Figure 10, are of the order of 20% and the average deviation is 5.6%. The results of this and other investigators as indicated previously in the deactivation study do not, however, justify a mechanism by which adsorbed ethylene is capable of reacting. In fact, Erkelens and Liefkens (*36*) recently concluded from their studies that the surface species of ethylene plays no role in the catalytic hydrogenation, confirming the work of other investigators (*35, 38, 39*). The Jenkins and Rideal mechanism, in which hydrogen is adsorbed on dual sites reacting with gas phase ethylene, but with no adsorption possible on that portion of the surface complexed with the ethylene, is probably most consistent with both conversion and deactivation data. By assuming that the total number of actives sites S_o reaches a steady state and that hydrogen adsorption controls the rate for the reactions

$$H_2 + Ni_2 \underset{k_2}{\overset{k_1}{\rightleftarrows}} 2Ni\,H \tag{17}$$

$$C_2H_4 + 2\,Ni\,H \xrightarrow{k_3} C_2H_6 + Ni_2 \tag{18}$$

an expression of the form

$$-r_B = k_1 k_3 S_o p_A p_B/(k_2 + k_3 p_B) \tag{19}$$

may be readily derived for the depletion rate of ethylene, which is comparable to the best fit form of Equation (16), but is in agreement with physical considerations as well. A similar form can be developed which includes the effect of a portion of the surface which is complexed with ethylene, if equilibrium is assumed for both hydrogen and ethylene adsorption. Possible differences in conditioning the catalyst surface in the studies of Jenkins and Rideal (*13*), Pauls et al. (*16*), and the current work might explain corresponding differences in the amount of complexing and, hence, reaction rates. In the former study, with pure ethylene used, the surface possibly became saturated with complexed ethylene, removing any future dependence on the ethylene concentration.

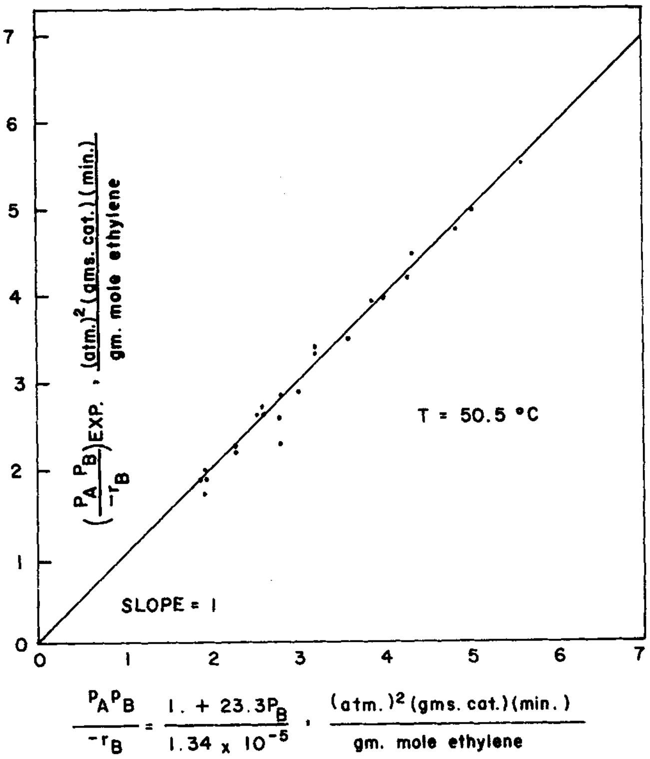

Fig. 10. Rate data correlation.

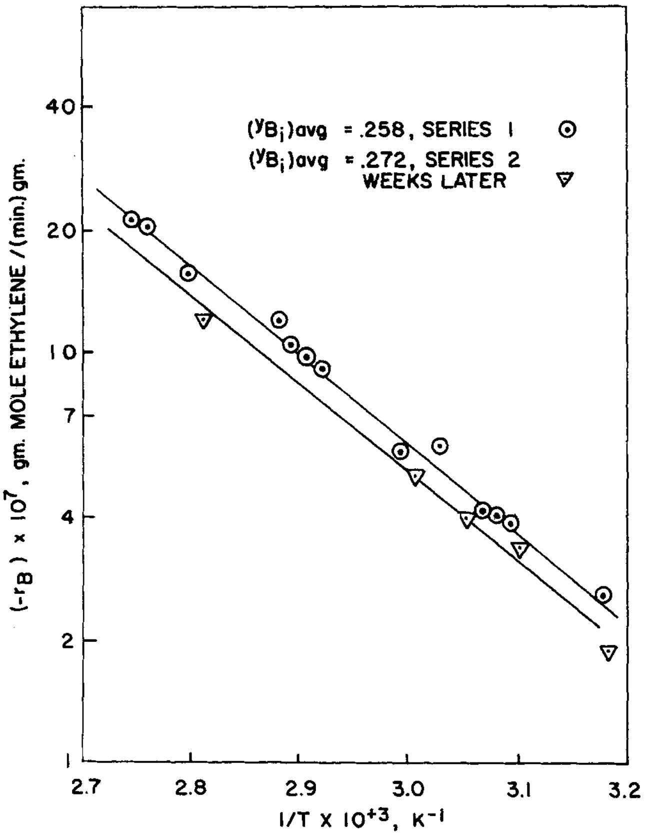

Fig. 9. Arrhenius plot for alumina catalyst.

Porocell Catalyst

Comparable tests were made in the reactor packed with 291 g. of activated bauxite catalyst (6.5 in.) and 510 g. of the glass beads to a covering height. The high surface area bauxite catalyst produced an activation energy of 5.25 kcal./mole for the reaction over the temperature range 27° to 90°C., indicating rate control by pore diffusion. In the packed-bed situation without fluidized beads, temperature differences of 40°C. in the lateral direction and 110°C. in the longitudinal direction were observed. Upon the addition of fluidized particles, typical differences were reduced to 5° and 10°C., respectively. The conversion level for the bed heights packed were too high to obtain initial rate data which is kinetically meaningful. By reducing the bed level and hence conversion, it is felt that the temperature control can be improved even more substantially. External temperatures may be held uniform, but localized unsteady internal temperature gradients might possibly exist in the highly porous catalyst. For further analysis and details of the porocell experiments, the reader is referred elsewhere (*37*).

CONCLUSIONS

Temperature gradients in a packed bed of large catalytic particles may be reduced to an acceptable level for kinetic analysis by fluidizing inert particles in the interstices.

The rate equation, including the activation energy, for the hydrogenation of ethylene over a nickel-on-alumina catalyst was found to be in reasonable agreement with literature values (*13*, *16*) on smaller particles. The catalyst apparently deactivated in the presence of ethylene and could be made more active by pretreating with hydrogen. The activity change in both instances is only temporary.

The deactivation and kinetic results support the postulate of an ethylene complex formation which is in equilibrium with gas-phase ethylene. The kinetic results are not able to differentiate between the postulated model and that of Jenkins and Rideal. Carbon-14 or comparable tracer techniques will be required to establish the precise mechanism.

ACKNOWLEDGMENT

The authors thank the National Science Foundation for helping to start the research with an Initiation Grant and the American Chemical Society, Petroleum Research Fund, for supporting the final year of study.

NOTATION

A, B, C = hydrogen, ethylene, and ethane, respectively
a = 5×10^{-4}, deactivation constant of Equation (14)
F_j = molar flow rate of component j at any position, g.-moles i/min.
F_o = total molar flow rate of gas at entrance, g.-moles/min.
F = total molar flow rate of gas at any position, g.-moles/min.
$f(c)$ = separated concentration dependence of reaction rate, units of r_j
$g(T)$ = separated temperature dependence of reaction rate, dimensionless
k_i = rate velocity constant for ith step units consistent with p_j and r_j
K = equilibrium constant, atm.$^{-1}$
p_j = partial pressure of component j, atm.
r_j = rate of formation of component j, g.-moles/g. of catalyst/min.
S_o = total active sites, number per gram of catalyst
t = on stream time, hr.
W = mass of catalyst, g.
Y_{ji} = mole fraction of component j at any position, and at entrance (input), respectively

LITERATURE CITED

1. Gabor, J. D., *Chem. Eng. Progr. Symp. Ser. No. 62*, **62**, 32 (1966).
2. Ishii, T., and G. L. Osberg, *AIChE J.*, **11**, 779 (1965).
3. Sabatier, P., and J. B. Senderens, *Compt. Rend.*, **124**, 1368 (1897).
4. Miyahara, K., *J. Res. Inst. Catal. Hokkaido Univ.*, **11**, 1 (1936).
5. Pease, R. N., "Equilibrium and Kinetics of Gas Reactions," Princeton Univ. Press, Princeton, N. J. (1942).
6. Rideal, E. K., *J. Chem. Soc. (London)*, **121**, 309 (1922).
7. Schuster, C., *Trans. Faraday Soc.*, **28**, 406 (1932).
8. Farkas, A., L. Farkas, and E. K. Rideal, *Proc. Roy. Soc.*, **A146**, 630 (1934).
9. Zur Strassen, H., *Z. Phys. Chem.*, **A169**, 81 (1934).
10. Toyama, O., *Rev. Phys. Chem. Japan*, **11**, 153 (1937).
11. *Ibid.*, **12**, 115 (1938).
12. Twigg, G. H., and E. K. Rideal, *Proc. Roy. Soc.*, **A171**, 55 (1939).
13. Jenkins, G. I., and E. K. Rideal, *J. Chem. Soc. (London)*, **1955**, 2490, 6 (1955).
14. Beeck, O., *Discussions Faraday Soc.*, **8**, 118 (1950).
15. Kemball, C., *J. Chem. Soc.*, **146**, 735 (1956).
16. Pauls, A. C., E. W. Comings, and J. M. Smith, *AIChE J.*, **5**, 453 (1959).
17. Miyahara, K., *J. Res. Inst. Catal. Hokkaido Univ.*, **14**, 134 (1966).
18. *Ibid.*, **14**, 144 (1966).
19. Tuul, J., and H. E. Farnsworth, *J. Am. Chem. Soc.*, **83**, 2253 (1961).
20. Crawford, E., M. W. Roberts, and C. Kemball, *Trans. Faraday Soc.*, **58**, 1761 (1962).
21. Twigg, G. H., *Discussions Faraday Soc.*, **8**, 79 (1950).
22. Eley, D. D., "Advances in Catalysis," Vol. 1, Academic Press, New York (1948).
22a. Schwab, G. M., *Z. Phys. Chem.*, **A171**, 421 (1934).
23. Palmer, D. M., and W. G. Palmer, *Proc. Roy. Soc. London*, **A99**, 402 (1921).
24. Conn, G. K. T., and G. H. Twigg, *ibid.*, **A171**, 70 (1939).
25. Beeck, O., A. E. Smith, and A. Wheeler, *ibid.*, **A177**, 62 (1940).
26. Turkevich, J., D. O. Schissler, and P. Irsa, *J. Phys. Coll. Chem.*, **55**, 1078 (1951).
27. Foss, J. G., and H. Eyring, *J. Phys. Chem.*, **62**, 103 (1958).
28. Cormack, D., S. J. Thomson, and G. Webb, *J. Catal.*, **10**, 1 (1958).
29. Horiuti, J., and M. Polanyi, *Trans. Faraday Soc.*, **30**, 1164 (1934).
30. Farkas, A., and L. Farkas, *J. Am. Chem. Soc.*, **60**, 22 (1938).
31. Farkas, A., *Trans. Faraday Soc.*, **35**, 906 (1939).
32. Eley, D. D., "Advances in Catalysis," Vol. 1, Academic Press, New York (1948).
33. Horiuti, J., and K. Miyahara, "National Standard Reference Data System," Natl. Bureau Standards, No. 13 (1968).
34. Ziegler, E. N., and W. T. Brazelton, *Ind. Eng. Chem. Progr. Develop.*, **2**, 276 (1963).
35. Eischens, R. P., and W. A. Pliskin, *Advan. Catalysis*, **10**, 1 (1958).
36. Erkelens, J., and Th. J. Liefkrens, *J. Catalysis*, **8**, 36 (1967).
37. Koestenblatt, S., Ph.D. thesis, Polytech. Inst., Brooklyn, N. Y. (1970).
38. Pliskin, W. A., and R. P. Eischens, *J. Chem. Phys.*, **24**, 492 (1956).
39. Morrow, B. A., and N. Sheppard, *ibid.*, **70**, 2406 (1966).

Manuscript received October 11, 1969; revision received March 2, 1970; paper accepted April 13, 1970. Paper presented at AIChE Atlanta meeting.